THE JOURNAL OF BIOLOGICAL CHEMISTRY VOL. 286, NO. 46, pp. 40069–40074, November 18, 2011

The Structure of the PDZ3-SH3-GuK Tandem of ZO-1 Protein Suggests a Supramodular Organization of the Membrane-associated Guanylate Kinase (MAGUK) Family Scaffold Protein Core*[S]

Received for publication, August 12, 2011, and in revised form, September 2, 2011 Published, JBC Papers in Press, September 30, 2011, DOI 10.1074/jbc.C111.293084

Lifeng Pan[‡1], **Jia Chen**[‡§1], **Jiang Yu**[‡1,2], **Haoyue Yu**[‡], **and Mingjie Zhang**[‡3]

From the [‡]*Division of Life Science, State Key Laboratory of Molecular Neuroscience, Molecular Neuroscience Center and the* [§]*Nano Science and Technology Program, Hong Kong University of Science and Technology, Clear Water Bay, Kowloon, Hong Kong*

Background: Every member of MAGUKs contains a sequentially organized PDZ-SH3-GuK tandem, although with unknown structural and functional implications.
Results: The structure of ZO-1 PDZ3-SH3-GuK reveals that PDZ and SH3-GuK form a structural and functional supramodule.
Conclusion: Formation of the PDZ-SH3-GuK supramodule may be a common feature of MAGUK scaffold proteins.
Significance: These findings can guide future functional studies of MAGUKs.

Membrane-associated guanylate kinases (MAGUKs) are a large family of scaffold proteins that play essential roles in tethering membrane receptors, adhesion molecules, and macromolecular signaling complexes for tissue developments, cell-cell communications, and intracellular signal transductions. The defining feature of the MAGUK family scaffolds is that each member contains a conserved core consisting of a PSD-95/Dlg/ZO-1 (PDZ) domain, an Src homology 3 (SH3) domain, and a catalytically inactive guanylate kinase (GuK) domain arranged in tandem, although the structural features and functional implications of the PDZ-SH3-GuK tandem arrangement are unclear. The structure of the ZO-1 PDZ3-SH3-GuK tandem solved in this study reveals that the PDZ domain directly interacts with the SH3-GuK module, forming a structural supramodule with distinct target binding properties with respect to the isolated domains. Structure-based sequence analysis suggests that the PDZ-SH3-GuK tandems of other members of the MAGUK family also form supramodules.

Membrane-associated guanylate kinases (MAGUKs)[4] were originally referred to as a group of cell junction proteins composed of synaptic scaffold protein PSD-95 from mammals, Dlg tumor suppressor from *Drosophila*, and tight junction protein ZO-1 from mammalian epithelia (1). MAGUKs are now known as a large family of scaffold proteins that play critical roles in diverse cellular processes including intercellular connections, cell polarity development and maintenance, neuronal plasticity, and cell survival in both metazoan and premetazoan (2–4). Despite the large differences in their lengths and amino acid sequences, every member of the MAGUK family of proteins except for membrane associated guanylate kinase inverted (MAGI) shares a core structural module composed of a PSD-95/Dlg/ZO-1 (PDZ) domain, an Src homology 3 (SH3) domain, and a catalytically inactive guanylate kinase (GuK) domain arranged sequentially into a PDZ-SH3-GuK tandem (see Fig. 1*A*). Recent studies have demonstrated that functional interaction between Dlg SH3-GuK tandem and its partner GuK-Holder is dependent on the presence of the upstream PDZ domain of Dlg and that this interaction is further regulated by the PDZ domain binding peptide (5, 6). Considering the highly conserved domain organization feature of MAGUKs throughout evolution, we hypothesized that the signature PDZ-SH3-GuK tandem of MAGUKs may form a structural supramodule with three domains interacting with each other to assemble into an integral structural unit, which has functions distinct from those of the isolated domains or the simple sum of the individual domains. We confirm this hypothesis here by presenting a detailed structural and biochemical characterization of the PDZ3-SH3-GuK tandem of ZO-1, which is a founding member of the PDZ as well as the MAGUK family of scaffold proteins. Furthermore, we provide evidence showing that the PDZ-SH3-GuK tandems in other members of the MAGUK family are likely to form structural supramodules as well.

EXPERIMENTAL PROCEDURES

Protein Expression and Purification—DNA fragments encoding human ZO-1 PDZ3 (residues 422–504), PDZ3 with C-terminal extension (residues 422–512), SH3-GuK (residues 506–812), and PDZ3-SH3-GuK (residues 422–888) were amplified by PCR using the full-length human ZO-1 cDNA (a gift from Alan Fanning, Department of Cell and Molecular

* This work was supported by Grants 663808, 664009, 660709, 663610, HKUST6/CRF/10, SEG_HKUST06, AoE/B-15/01-II, and AoE/M-04/04 from the Research Grants Council of Hong Kong (to M. Z.).
The atomic coordinates and structure factors (codes 3SHU and 3SHW) have been deposited in the Protein Data Bank, Research Collaboratory for Structural Bioinformatics, Rutgers University, New Brunswick, NJ (http://www.rcsb.org/).
[S] The on-line version of this article (available at http://www.jbc.org) contains supplemental Table 1 and Figs. S1–S4.
[1] These authors contributed equally to this work.
[2] Present address: School of Physics, the University of New South Wales, Sydney 2052, Australia.
[3] To whom correspondence should be addressed. Tel.: 852-2358-8709; Fax: 852-2358-1552; E-mail: mzhang@ust.hk.
[4] The abbreviations used are: MAGUK, membrane-associated guanylate kinase; GuK, guanylate kinase; ITC, isothermal titration calorimetry; Cx45, connexin 45; DLG, disc-large.

Physiology, University of North Carolina at Chapel Hill, accession number NM_003257) as the template and cloned into an in-house modified version of pET32a vector. Various mutants of ZO-1 PDZ3-SH3-GuK were created using standard PCR-based methods. Recombinant proteins were expressed in BL21 (DE3) *Escherichia coli* cells at 16 °C. His_6-tagged ZO-1 fragment proteins expressed in bacterial cells were purified by Ni^{2+}-nitrilotriacetic acid-agarose (Qiagen) affinity chromatography followed by size-exclusion chromatography. The N-terminal His_6 tag of each recombinant protein was cleaved by protease 3C and removed by size-exclusion chromatography.

Crystallization, Data Collection, and Structure Determination—The crystal of ZO-1 PDZ3 (10.0 mg/ml in 20 mM Tris-HCl buffer, 100 mM NaCl, pH 7.5) was grown using the hanging-drop method by mixing 1 μl of protein sample with an equal volume of 20% (w/v) PEG4000, 10% (v/v) 2-propanol, and 0.1 M HEPES, pH 7.5, at 16 °C. Crystals were transferred to the reservoir solution containing 15% (v/v) glycerol as the cryoprotectant and flash-cooled with liquid nitrogen. Diffraction data were collected at 110 K on a Rigaku RAXIS IV++ imaging plate system with a MicroMax-007 copper rotating anode generator. The diffraction data were processed and scaled using the programs MOSFLM (7) and SCALA in the CCP4 suite (8). The ZO-1 PDZ3 structure was solved by the molecular replacement method with the program Phaser (9) using the structure of PSD-95 PDZ3 (Protein Data Bank (PDB) code 1TP3) as the search model. ZO-1 PDZ3-SH3-GuK (15.0 mg/ml in 20 mM Tris-HCl buffer, 100 mM NaCl, pH 7.5) was mixed with the Cx45 peptide with a molar ratio of 1:5 followed by crystallization using the hanging-drop method by mixing 1 μl of protein sample with an equal volume of 16% (w/v) PEG 8000, 0.1 sodium citrate, pH 5.5. Crystals were dehydrated by serial transfer to a solution of increasing PEG 8000 concentration up to 30% and flash-frozen with liquid nitrogen. The diffraction data were collected at the Shanghai Synchrotron Radiation Facility (SSRF) beamline BL17U at a wavelength of 0.979 Å and at 100 K. The diffraction data were processed and scaled using HKL2000 package (10). The ZO-1 PDZ3-SH3-GuK·Cx45 complex structure was solved by the molecular replacement using the structures of ZO-1 PDZ3 and PSD-95 SH3-GuK (PDB code 1KJW) as the search models. Structures were fitted and rebuilt with the program Coot (11) and refined with REFMAC5 (12) and CNS (13). The overall qualities of the structural models were assessed using PROCHECK (14). The data processing and refinement statistics are summarized in supplemental Table S1.

Fluorescence Polarization Assay—Fluorescence anisotropy binding assays were performed on a PerkinElmer Life Sciences LS-55 fluorometer equipped with an automated polarizer at 25 °C. FITC-labeled Jam1 and Cx45 peptides were commercially synthesized, and the purities of the peptides were >95%. Fluorescence titration was performed with additions of increasing amounts of ZO-1 PDZ3 or PDZ3-SH3-GuK to a constant concentration of FITC-labeled peptide (~1 μM). The titration curves were fitted with ORIGIN version 5.0 (MicroCal) software package using nonlinear least squares fitting, assuming a one-site binding model.

Isothermal Titration Calorimetry—ITC was carried out on a MicroCal VP-ITC microcalorimeter at 25 °C. All measurements were collected by titration of peptides into protein solutions. Proteins and peptides were dissolved in a buffer composed of 50 mM Tris, 100 mM NaCl (pH 7.5). All solutions were degassed for 5–10 min without stirring and kept on ice before the ITC experiments. For all ITC experiments, protein sample (100 μM) was placed in the sample chamber (~2 ml), whereas the peptide solution (1 mM) was transferred into a 250-μl injection syringe. Each titration experiment comprised a single 2-μl injection followed by 10-μl injections at 180-s intervals. The data from each experiment were collected and analyzed using ORIGIN. Thermodynamic parameters were determined using nonlinear least squares fitting, assuming a one-site binding model.

RESULTS AND DISCUSSION

We determined the 2.9 Å resolution crystal structure of ZO-1 PDZ3-SH3-GuK in complex with a peptide composed of the extreme C-terminal 10 residues of connexin 45 (referred to as the Cx45 peptide, a highly preferred ZO-1 PDZ3 target identified in a phage display-based screening (15) (supplemental Table 1)). The most important feature of the ZO-1 PDZ3-SH3-GuK tandem structure is that its three domains indeed physically interact with each other, forming an integrated supramodule with a rod-like shape (Fig. 1*B*). In this supramodule, the SH3 and GuK domains interact with each other through the fifth strand of the SH3 domain and the strand following the GuK domain, forming an integrated structural unit, as shown previously for the isolated ZO-1 SH3-GuK (16) and the SH3-GuK modules of ZO-3 (PDB 3KFV) and PSD-95 (17, 18) (Fig. 1*B*, supplemental Fig. S3, *A–D*). Therefore, we do not discuss this interaction any further here. The PDZ3 domain in the PDZ3-SH3-GuK tandem contains an additional amphipathic α-helix (αC) at its C terminus (Fig. 1*B*). The hydrophobic face of this helix packs with an otherwise exposed hydrophobic surface (formed by residues from βB_{PDZ3} and βC_{PDZ3}) distant from the target binding groove of the PDZ domain (Fig. 2, *A* and *C*). Several recent PDZ domain structures (19, 20), together with our bioinformatics survey (21), indicate that a large portion of PDZ domains is likely to have structured extensions beyond the canonical domain boundaries of the domains and that such extensions can actively modify the ligand binding properties of PDZ domains. However, in this case, we did not detect obvious differences in Cx45 peptide binding affinities with or without this extended α-helix (supplemental Fig. S4).

What is shown for the first time from the ZO-1 PDZ3-SH3-GuK structure is that the PDZ3 domain extensively interacts with one side of the SH3 domain (Fig. 1*B*). Specifically, a number of residues from αB, the βB/βC-loop of PDZ3, and the short inter-PDZ3/SH3 linker interact with several residues from the SH3 domain, such as the $Phe519_{SH3}$ from βA_{SH3}, $Trp557_{SH3}$ from βC_{SH3}, and $Asn576_{SH3}$ preceding αA_{SH3} (Fig. 2, *A* and *B*, supplemental Fig. S1). The inter-PDZ3/SH3 packing is mainly mediated by hydrogen bonds and charge-charge interactions (*e.g.* a strong interdomain salt bridge formed between $Arg480_{PDZ3}$ and $Asp547_{SH3}$ with a distance of 2.8 Å and a number of hydrogen bonds formed by the side chain of Asp-517 from the interdomain linker and the backbones of $Asn441_{PDZ3}$, $Arg480_{PDZ3}$, and $Thr548_{SH3}$). Additional

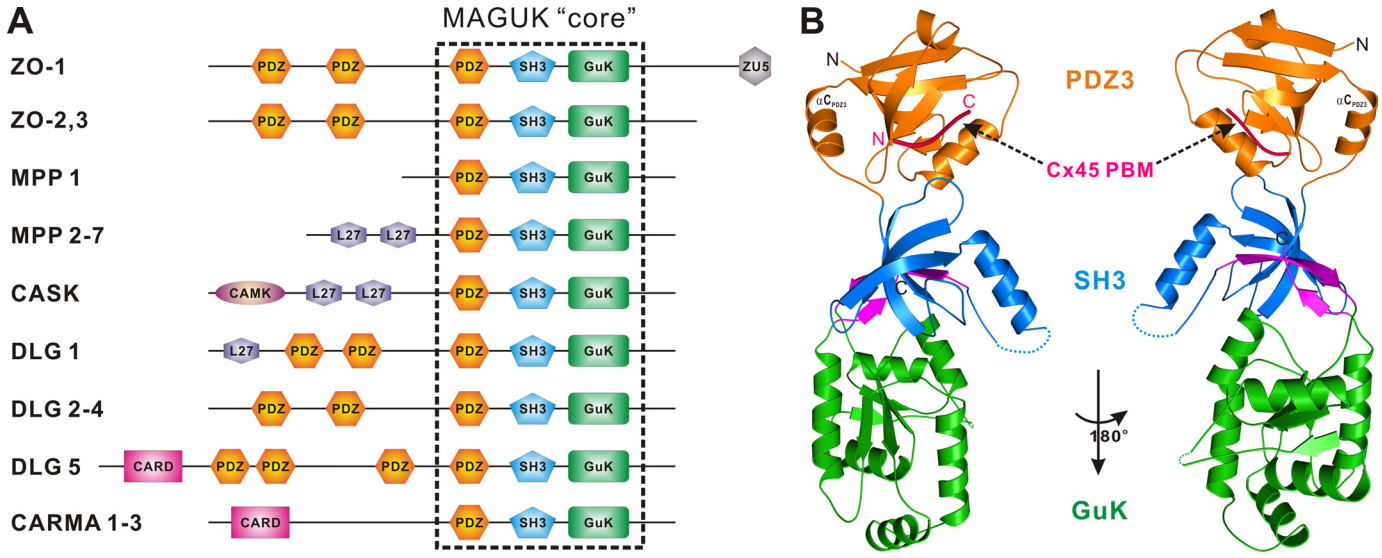

FIGURE 1. **Domain organizations of MAGUK proteins and the overall structure of the ZO-1 PDZ3-SH3-GuK·Cx45 peptide complex.** *A*, a schematic diagram showing the domain organizations of selected MAGUK proteins with the conserved PDZ3-SH3-GuK core highlighted with a *dashed square*. *CAMK*, Ca^{2+}/calmodulin-dependent protein kinase; *CARD*, caspase activation and recruitment domain. *B*, ribbon diagram showing the overall structure of the ZO-1 PDZ3-SH3-GuK·Cx45 peptide complex. In this drawing, the PDZ3 domain is shown in *orange*, the SH3 domain is in blue, the GuK domain is in *green*, the fifth strand of the SH3 domain and the strand following the GuK domain are in *magenta*, and the bounded Cx45 peptide is in *pink*. *PBM*, protein binding motif.

hydrophobic contacts further stabilize the inter-PDZ3/SH3 interaction (*e.g.* the side chain of $Ile479_{PDZ3}$ binds to a pocket formed by $Phe519_{SH3}$, $Thr548_{SH3}$, and $Trp557_{SH3}$) (Fig. 2*B*). Importantly, the residues responsible for the inter-PDZ3/SH3 interactions are highly conserved in ZO-1 (supplemental Fig. S1), indicating that the observed PDZ3/SH3 interaction in mammalian ZO-1 is likely to be a conserved feature of ZO-1 in other species.

We further analyzed the amino acid sequences of other members of MAGUKs with that of ZO-1. This analysis revealed that the caspase recruitment domain containing MAGUK (CARMA) family MAGUKs as well as DLG5 are likely to have the similar PDZ-SH3-GuK supramodular organization as these MAGUKs contain equivalent residues responsible for the inter-PDZ/SH3 interactions observed in the ZO-1 PDZ3-SH3-GuK structure (*e.g.* Asn-441, Glu-481, Asp-517, Asp-547, Thr-548, and Trp-557; supplemental Fig. S2). It is not clear simply based on the sequence analysis whether the PDZ-SH3-GuK tandems in the membrane palmitoylated protein (MPP) family and in DLG1–4 MAGUKs also form supramodules due to their amino acid sequence diversities. However, several previously reported studies have indicated that the PDZ-SH3-GuK tandems in the DLG family MAGUKs indeed form functional supramodules. For example, the interaction between the GuK domain of *Drosophila* DLG and its target GuK-Holder requires both PDZ3 and the short linker connecting PDZ3 and SH3. Deletion of or replacement of the PDZ3/SH3-linker with flexible residues diminishes the GuK-mediated binding to GuK-Holder (5). Additionally, binding of a target peptide to PDZ3 weakens the GuK-Holder binding ability of the SH3-GuK module, implying a conformational coupled allosteric regulation between PDZ3 and SH3-GuK (6). In another example, the interaction of the GuK domain of mammalian PSD-93/DLG2 to MAP1a is also allosterically regulated by its PDZ3, albeit in this case, binding of the PDZ ligands releases its inhibition of the GuK/MAP1a interaction (22). Therefore, the supramodular organization of the PDZ-SH3-GuK tandem seen in ZO-1 is likely to be a general property for at least some members of MAGUKs.

The structure of the PDZ3-SH3-GuK tandem also reveals that the target binding pocket of ZO-1 PDZ3 (*i.e.* the αB/βB-groove) is significantly altered by the packing of the SH3 domain as well as the short linker connecting the PDZ3 and SH3 domains (Fig. 2*A*). Specifically, the bulky hydrophobic Leu-549 and Leu-554 residues from the βB/βC-loop of the SH3 domain interact with Val-484 and Leu-485 from PDZ3 αB, forming the hydrophobic binding pocket accommodating Val(−2) from the Cx45 peptide (Fig. 3, *A* and *B*). The three residues from the inter-PDZ3/SH3 linker (^{516}GDS^{518}) together with Phe-519 from βA_{SH3} interact extensively with the βB/βC-loop and the N-terminal end of αB of PDZ3, thus creating a wall at the one end of the target binding αB/βB-groove of PDZ3 (Fig. 3, *A* and *B*). Consistent with this structural feature, the Cx45 peptide is not able to form an antiparallel β-sheet with the βB strand of PDZ3. Instead, the last three residues of the peptide insert vertically into the hydrophobic pocket formed by residues from both the PDZ3 and the SH3 domains (Fig. 3*B*). This structural analysis immediately suggests that the two forms of ZO-1 PDZ3, one in its isolated state and the other in the PDZ3-SH3-GuK tandem, are likely to have very different target binding affinities, although the overall conformations of PDZ3 in the two forms are highly similar (supplemental Fig. S3*E*). We further predict that the extensive hydrophobic contacts between Val(−2) of Cx45 and the four hydrophobic residues from PDZ3 and SH3 should enhance the binding between Cx45 and the PDZ3-SH3-GuK tandem. Exactly as predicted, the Cx45 peptide binds to the PDZ3-SH3-GuK tandem with a K_d value of ~7.9 μM, whereas the binding of the peptide to the isolated PDZ3 is much weaker (K_d of ~72 μM; Fig. 4*A*) and no binding is detectable between the peptide and SH3-GuK tan-

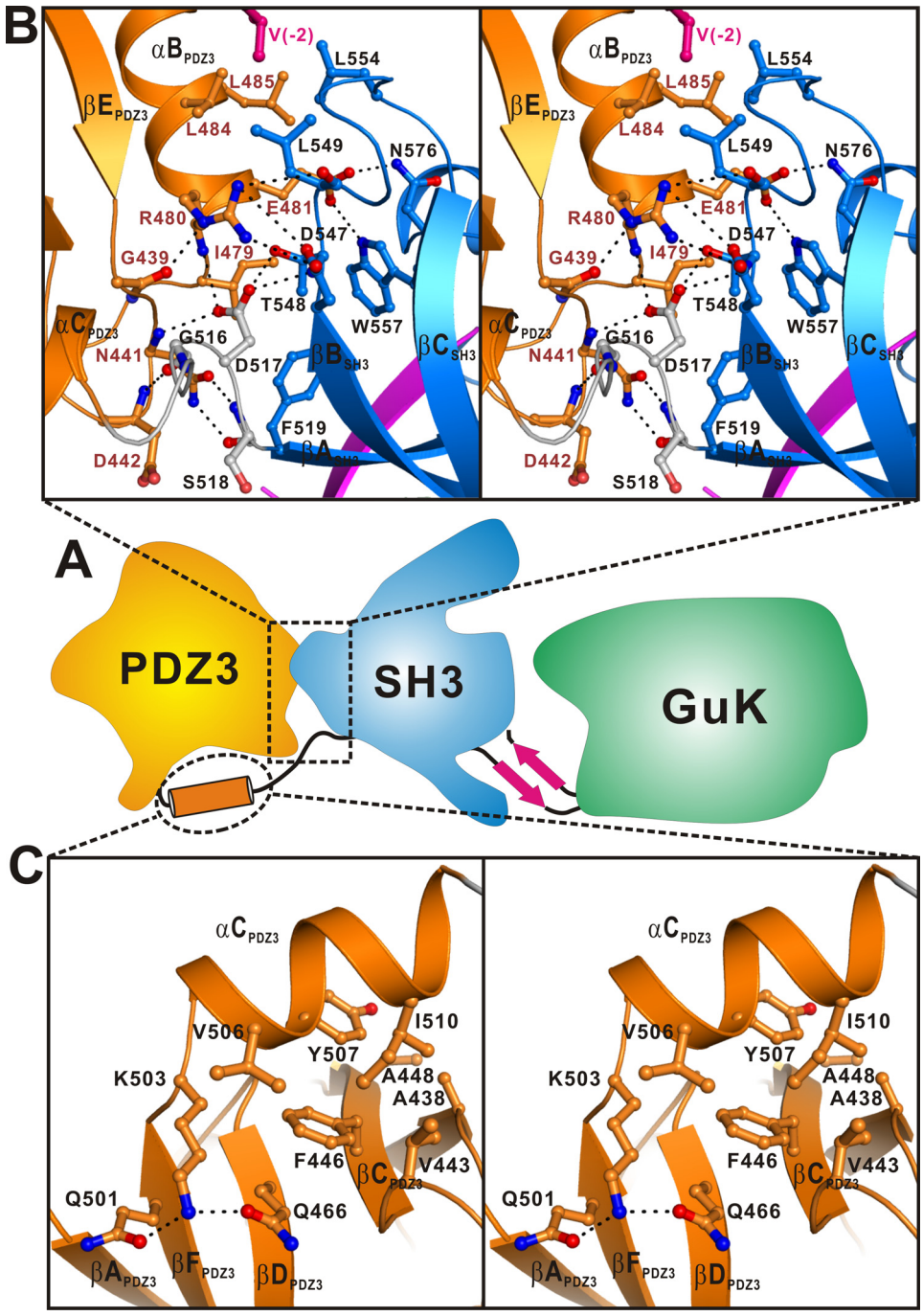

FIGURE 2. **Details of the PDZ3-SH3 interface and PDZ3/C-terminal α-helix extension interaction.** *A*, a schematic diagram summarizing the overall architecture of the ZO-1 PDZ3-SH3-GuK supramodule. *B*, stereo view showing the detailed interactions between the PDZ3 and SH3 interface. The color scheme is the same as in Fig. 1*B* except that the short interdomain linker between PDZ3 and SH3 is shown in *gray*. *C*, stereo view of the interaction between PDZ3 and its C-terminal α-helix extension. The hydrogen bonds and salt bridges are indicated as *dashed lines*. The interacting residues are shown in the *stick model*.

dem, suggesting that the increased affinity comes from the newly generated PDZ3-SH3 interface rather than isolated domains. To further prove that the PDZ3-SH3 interface generated an additional binding groove for PDZ3 binding peptide, we substituted Leu-549 in the βB/βC-loop of the SH3 domain with an Arg, and this substitution is expected to disrupt the interdomain interaction between PDZ3 and SH3 based on the structure of PDZ3-SH3-GuK shown in Fig. 2*B*. Interestingly, the L549R mutant of PDZ3-SH3-GuK displayed a much weaker binding to the Cx45 peptide (K_d of ~62 μM; Fig. 4*C*), supporting our notion that the interaction between PDZ3 and SH3 modifies the target binding property of ZO-1 PDZ3. The enhanced target peptide binding of PDZ3 afforded by the formation of the PDZ3-SH3-GuK supramodule is also observed for Jam1, another reported ZO-1 PDZ3 binding target (23, 24). Isolated ZO-1 PDZ3 or SH3-GuK tandem has essentially no detectable binding to the carboxyl peptide of Jam1. In contrast, the PDZ3-SH3-GuK tandem binds to the Jam1 peptide with a K_d of ~51

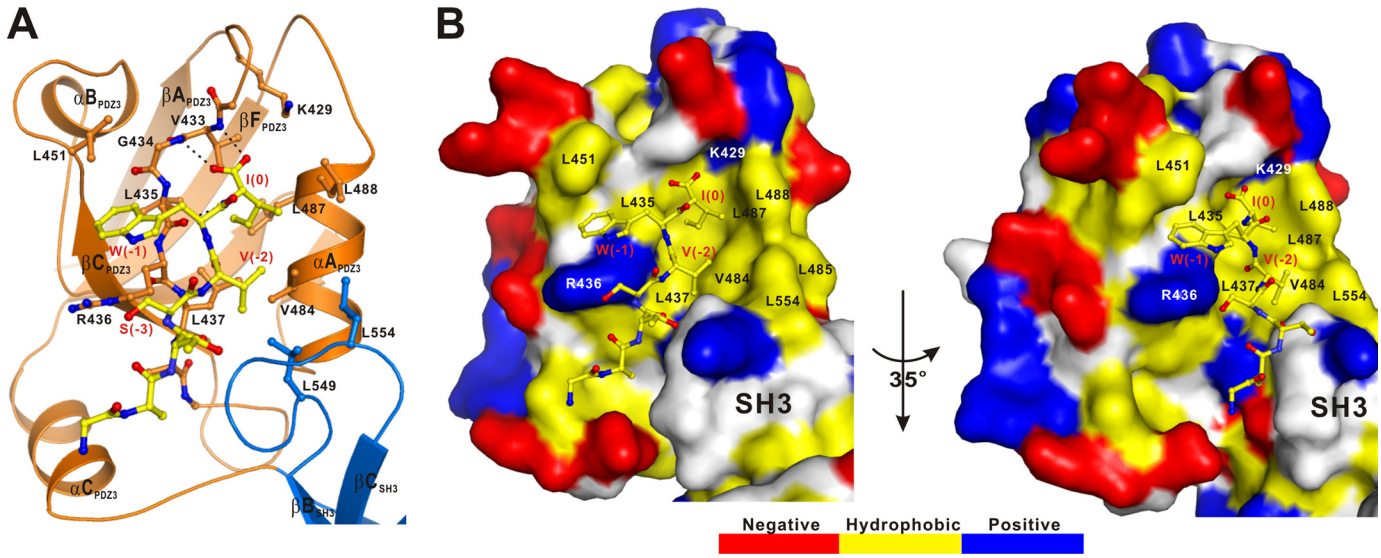

FIGURE 3. **Molecular details of the ZO-1 PDZ3-SH3-GuK and Cx45 peptide interaction.** *A*, stick and ribbon representation showing the molecular details of the Cx45 peptide binding to the PDZ3-SH3-GuK tandem. *B*, the combined surface representation and the stick model showing the interaction interface between ZO-1 PDZ3-SH3-GuK and the Cx45 peptide. In this presentation, the PDZ3-SH3-GuK tandem is shown in the surface model, and the Cx45 peptide is shown in the stick model. The hydrophobic amino acid residues are drawn in *yellow*, the positively charged residues are in *blue*, the negatively charged residues are in *red*, and the uncharged polar residues are in *gray*.

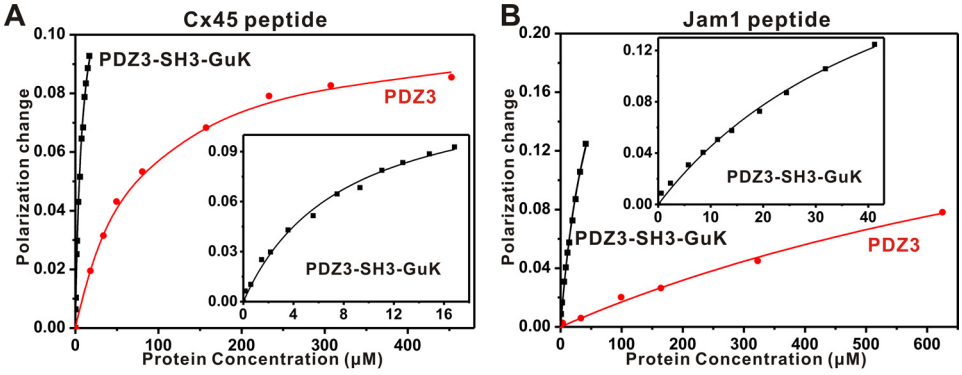

C

Kd(μM)	PDZ3	SH3-GuK	PDZ3-SH3-GuK	PDZ3-SH3-GuK (L549R)
Cx45	72±6	not detectable	8±1	63±14
Jam1	not detectable	not detectable	51±7	not detectable

FIGURE 4. **Isolated PDZ3 and PDZ3 in the PDZ3-SH3-GuK tandem have distinct target binding properties.** *A* and *B*, fluorescence-based measurements of the binding affinities of ZO-1 PDZ3 and the PDZ3-SH3-GuK to the Cx45 peptide (*A*) and the Jam1 peptide (*B*). The *inset* in each panel shows an expanded binding curve of the PDZ3-SH3-GuK tandem to the Cx45 peptide and the Jam1 peptide, respectively. *C*, the binding affinities between various forms of ZO-1 proteins and the Cx45 peptide or Jam1 peptide derived from the fluorescence-based binding assays.

μM (Fig. 4*B*). Similarly, the substitution of Leu-549 with Arg essentially abolished the Jam1 peptide binding of the PDZ3-SH3-GuK tandem (Fig. 4*C*). Altogether, these two lines of evidences suggested that the PDZ3-SH3 interface could help potentiate the peptide binding ability of PDZ3 domain and that disruption of the packing interface would reverse this affinity enhancement.

In summary, the structure of the PDZ3-SH3-GuK tandem of ZO-1, a founding member of the MAGUK family, reveals that the PDZ3 domain physically interacts with the SH3 domain in the SH3-GuK module, and thus the three domains fold together, forming a structural and functional supramodule. In addition to elucidating the first atomic mechanism for the formation of PDZ-SH3-GuK supramodule, we further provide evidence indicating that formation of the PDZ-SH3-GuK supramodule is likely to be a common feature for a number of other MAGUK family scaffold proteins.

Acknowledgments—We thank Dr. Yanxiang Zhao for providing the in-house x-ray diffraction machine and the BL17U1 beamline of the Shanghai Synchrotron Radiation Facility for the x-ray beam time.

REFERENCES

1. Woods, D. F., and Bryant, P. J. (1993) *Mech. Dev.* **44,** 85–89
2. de Mendoza, A., Suga, H., and Ruiz-Trillo, I. (2010) *BMC Evol. Biol.* **10,** 93
3. te Velthuis, A. J., Admiraal, J. F., and Bagowski, C. P. (2007) *BMC Evol. Biol.* **7,** 129
4. Funke, L., Dakoji, S., and Bredt, D. S. (2005) *Annu. Rev. Biochem.* **74,** 219–245
5. Qian, Y., and Prehoda, K. E. (2006) *J. Biol. Chem.* **281,** 35757–35763

6. Newman, R. A., and Prehoda, K. E. (2009) *J. Biol. Chem.* **284,** 12924–12932
7. Leslie, A. G. (1992) *Joint CCP4 + ESF-EAMCB Newsletter on Protein Crystallography*, Vol. **26**, Collaborative Computational Project No. 4, Daresbury Laboratory, Daresbury, UK
8. Collaborative Computational Project, Number 4 (1994) *Acta Crystallogr. D. Biol. Crystallogr.* **50**, 760–763
9. McCoy, A. J., Grosse-Kunstleve, R. W., Adams, P. D., Winn, M. D., Storoni, L. C., and Read, R. J. (2007) *J. Appl. Crystallogr.* **40,** 658–674
10. Otwinowski, Z., and Minor, W. (1997) *Methods Enzymol.* **276,** 307–326
11. Emsley, P., and Cowtan, K. (2004) *Acta Crystallogr. D. Biol. Crystallogr.* **60,** 2126–2132
12. Murshudov, G. N., Vagin, A. A., and Dodson, E. J. (1997) *Acta Crystallogr. D. Biol. Crystallogr.* **53,** 240–255
13. Brünger, A. T., Adams, P. D., Clore, G. M., DeLano, W. L., Gros, P., Grosse-Kunstleve, R. W., Jiang, J. S., Kuszewski, J., Nilges, M., Pannu, N. S., Read, R. J., Rice, L. M., Simonson, T., and Warren, G. L. (1998) *Acta Crystallogr. D. Biol. Crystallogr.* **54,** 905–921
14. Laskowski, R. A., Moss, D. S., and Thornton, J. M. (1993) *J. Mol. Biol.* **231,** 1049–1067
15. Tonikian, R., Zhang, Y., Sazinsky, S. L., Currell, B., Yeh, J. H., Reva, B., Held, H. A., Appleton, B. A., Evangelista, M., Wu, Y., Xin, X., Chan, A. C., Seshagiri, S., Lasky, L. A., Sander, C., Boone, C., Bader, G. D., and Sidhu, S. S. (2008) *PLoS Biol.* **6,** e239
16. Lye, M. F., Fanning, A. S., Su, Y., Anderson, J. M., and Lavie, A. (2010) *J. Biol. Chem.* **285,** 13907–13917
17. McGee, A. W., Dakoji, S. R., Olsen, O., Bredt, D. S., Lim, W. A., and Prehoda, K. E. (2001) *Mol. Cell* **8,** 1291–1301
18. Tavares, G. A., Panepucci, E. H., and Brunger, A. T. (2001) *Mol. Cell* **8,** 1313–1325
19. Petit, C. M., Zhang, J., Sapienza, P. J., Fuentes, E. J., and Lee, A. L. (2009) *Proc. Natl. Acad. Sci. U.S.A.* **106,** 18249–18254
20. Yan, J., Pan, L., Chen, X., Wu, L., and Zhang, M. (2010) *Proc. Natl. Acad. Sci. U.S.A.* **107,** 4040–4045
21. Wang, C. K., Pan, L., Chen, J., and Zhang, M. (2010) *Protein Cell* **1,** 737–751
22. Brenman, J. E., Topinka, J. R., Cooper, E. C., McGee, A. W., Rosen, J., Milroy, T., Ralston, H. J., and Bredt, D. S. (1998) *J. Neurosci.* **18,** 8805–8813
23. Ebnet, K., Schulz, C. U., Meyer, Zu., Brickwedde, M. K., Pendl, G. G., and Vestweber, D. (2000) *J. Biol. Chem.* **275,** 27979–27988
24. Itoh, M., Sasaki, H., Furuse, M., Ozaki, H., Kita, T., and Tsukita, S. (2001) *J. Cell Biol.* **154,** 491–497